

Nanofluidic channels fabricated by e-beam lithography and polymer reflow sealing

Mina Fouad, Mustafa Yavuz,^{a)} and Bo Cui^{b)}

Waterloo Institute for Nanotechnology (WIN), University of Waterloo, Waterloo, Ontario N2L3G1, Canada

(Received 9 July 2010; accepted 25 October 2010; published 29 November 2010)

The authors developed a facile approach for creating nanofluidic channels by electron beam lithography that used a bilayer e-beam resist consisting of poly(methyl methacrylate) (PMMA) on top of poly(dimethyl glutarimide) (PMGI). In the process, the more sensitive PMGI was fully exposed with channel patterns, and the less sensitive PMMA was only fully exposed with a chain of dot patterns right above the channel patterns. PMMA was then developed to form a chain of holes through which PMGI channels were developed. After closing the holes by thermal reflowing PMMA, channels in PMGI were sealed with PMMA. The current method is capable of fabricating simultaneously channels with different channel widths. © 2010 American Vacuum Society. [DOI: 10.1116/1.3517620]

I. INTRODUCTION

Nanofluidics is of considerable interest for many applications, such as DNA analysis,¹ as well as for the study of transport phenomena in the nanoscale.² Fabrication of nanochannels consists of trench patterning and its sealing afterward.³ E-beam lithography (EBL), nanoimprint lithography (NIL), laser interference lithography, and focused ion beam etching are typically used to fabricate the nanoscale trenches. Once the trenches are created, various sealing techniques have been employed to form sealed nanofluidic channels.

The most straightforward channel-sealing method is by wafer bonding. For instance, Han and Craighead fabricated nanochannels (here, only the height of the channels was in the nanoscale) using conventional photolithography and then sealed them by another wafer using anodic wafer bonding.⁴ However, such a sealing process involves high temperature and high voltage. Cao *et al.* fabricated nanofluidic channels by NIL and sealed them by sputter deposition of oxide that coated both the trench bottom and the sidewall.⁵ Although the method is rather straightforward, it can only seal trenches of a certain high aspect ratio; as otherwise, the trench might be filled up by the oxide before forming a channel. In addition, the channels so formed have an irregular shape depending on the height and width of the trench and the arrival angle distribution of sputtered materials. Chen *et al.* demonstrated trench patterning using laser interference lithography and sealing them using thermal oxidation of silicon due to the slower oxide growth at the concave corners than flat surfaces.⁶ This method, however, also requires trenches of a certain high aspect ratio, and it involves long oxidation times at high temperatures. Recently, Xia *et al.* fabricated nanofluidic channels in Si using NIL and then sealed them using pulsed laser melting of Si.⁷ The sealing is achieved because the nanosecond pulsed laser only melts and reflows the Si on

the upper part of the ridges that collapse and are “welded” together. Clearly, such method works only for narrow (considerably less than the wavelength, so light does not reach the trench bottom) trenches that are deep (much deeper than the thermal penetration depth of Si for the duration of the pulse). Devlin *et al.* fabricated nanochannels by electron beam lithography using a negative resist based on polynorborene.⁸ After development, the resist lines were coated with a hard cap layer, through which the resist can evaporate when heated to a decomposition temperature of above 400 °C. While this method is very simple, the relatively high annealing temperature makes it difficult to be integrated into microfluidic systems using soft materials such as polydimethylsiloxane.

Here, we report the fabrication of nanochannels by e-beam lithography and thermal reflow of the sealing polymer. Compared to the methods mentioned above, the current process is a simple one that does not involve a high temperature process, and it is able to fabricate nanochannels of different widths and aspect ratios.

II. FABRICATION

The process used bilayer e-beam resists consisting of poly(methyl methacrylate) (PMMA) on top of poly(dimethyl glutarimide) (PMGI, MicroChem Corporation). The channels were defined in PMGI that is more sensitive to e-beam exposure than PMMA, and sealed by reflowing PMMA, the glass transition temperature of which is significantly lower than that of PMGI (189 °C). Figure 1 shows a schematic fabrication process. To prepare the substrate for electron beam lithography, the wafer was cleaned using acetone and 2-propanol before spin-coating a layer of antireflection coating (ARC, XHRiC from Brewer Sciences) that was subsequently baked at 180 °C for 2 min to cross-link it. Here, the ARC acted as an adhesion layer for PMGI, as it was found that the base developer for PMGI can penetrate easily underneath PMGI and lifted it off when it was coated directly on a bare silicon wafer. PMGI (70 nm) and PMMA (170 nm)

^{a)}Electronic mail: myavuz@mecheng1.uwaterloo.ca

^{b)}Electronic mail: bcui@uwaterloo.ca

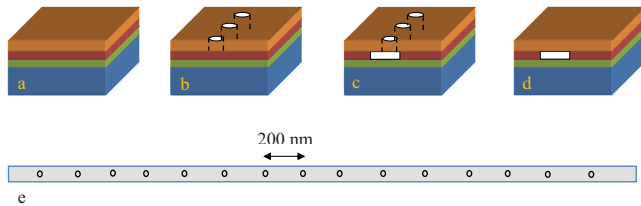


FIG. 1. (Color online) Schematic process for the fabrication of sealed nanofluidic channels. (a) Preparation of the substrate consisting of bilayer resists on an ARC layer; (b) e-beam exposure and development of PMMA that resulted in a sub-50-nm hole array; (c) development of PMGI through the holes in PMMA; and (d) PMMA thermal reflow to close the holes, leading to sealed channels. (e) Shows the CAD pattern where the long rectangle is set an area dose of 120–160 $\mu\text{C}/\text{cm}^2$ depending on the channel width, and the chain of dots is set with a point dose of 8.5 fC.

were then spin-coated on ARC and baked on a hotplate at 200 °C for 3 and 10 min, respectively. Next, the bilayer resist was exposed using a LEO 1530 scanning electron microscope (SEM) equipped with a nanometer pattern generation system and a beam blanker. The EBL was carried out with 20 kV acceleration voltage and 120 pA beam current. The computer-aided design (CAD) pattern for a single channel is shown in Fig. 1(e), where the long channel uses a low area dose (120–160 $\mu\text{C}/\text{cm}^2$ depending on channel width) that can fully expose the bottom PMGI layer but not the top PMMA layer, and the dots use a high point dose of 8.5 fC to fully expose PMMA (and apparently the more sensitive PMGI below it). Here, the dose for PMGI is higher than its sensitivity of 50–100 $\mu\text{C}/\text{cm}^2$ because the channel is narrower than the range of backscattered electrons, and thus, it is less exposed by backscattered electrons than the case of large area exposure.

After e-beam exposure, the development of PMMA was carried out using methyl isobutyl ketone (MIBK):2-propanol=1:3 for 20 s, which resulted in a hole array with sub-50-nm diameter in PMMA. Next, PMGI channels were developed using 1:1 diluted (with de-ionized water) AZ 300 MIF developer [contains 2.4% tetramethylammonium hydroxide (TMAH)] for 5 min in a low-power ultrasonic bath. It was found that such a long development time with ultrasonic agitation was needed in order to dissolve the exposed PMGI under PMMA, presumably because of the inefficiency of developer transport through the nanoholes in PMMA. Finally, the holes in PMMA were closed, and thus, the channels were sealed by baking the sample on a hotplate at 150 °C for 40 s.

III. RESULTS AND DISCUSSION

Figure 2 shows SEM images of a chain of holes in PMMA by EBL, the channels in PMGI after development through the holes, and the completed sealed nanochannel after PMMA thermal reflow. Figure 3 shows sealed channels of various widths from 150 to 450 nm with channel height of 70 nm, which is equal to the thickness of the PMGI layer. We found that the channels were wider than the CAD pattern by 50–100 nm, owing to the proximity effect that leads to exposure of areas close to the primary beam, and the fact that

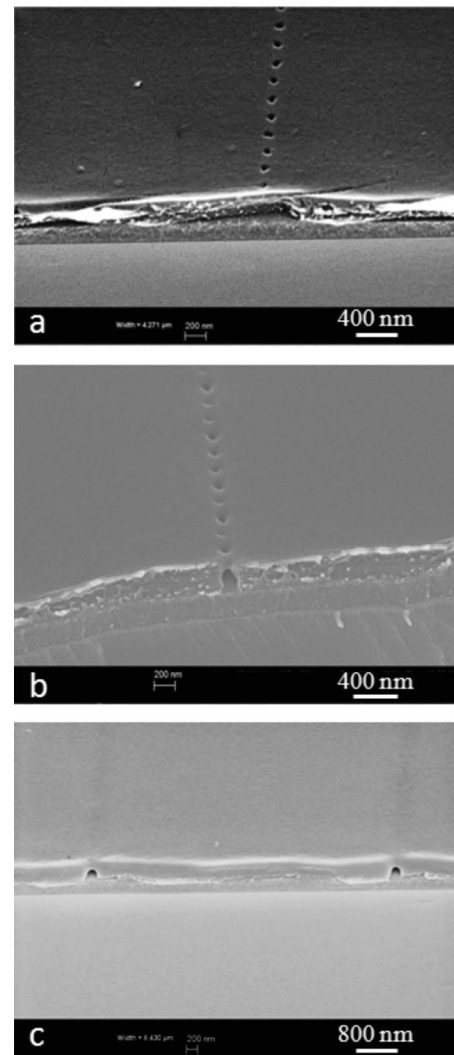


FIG. 2. SEM images taken after (a) e-beam exposure and development of PMMA that resulted in a sub-50-nm hole array; (b) development of PMGI through the holes in PMMA; and (c) PMMA thermal reflow to close the holes, leading to sealed channels.

PMGI can be dissolved by the basic aqueous developer even when unexposed. Nonetheless, the channel widths were still roughly determined by the CAD pattern because the exposed PMGI develops much faster than the unexposed one.

In principle, the current process can achieve channels well below 100 nm wide if one could find a suitable resist having higher resolution than PMGI. Here, we chose PMGI and PMMA as the bilayer resist materials because (1) PMGI is more sensitive than PMMA; (2) it is resistant to the solvent and developer used for PMMA; (3) with a glass transition temperature of 189 °C, it is stable at the annealing temperature of ~ 150 °C; and (4) its developer does not attack PMMA. Unlike PMMA, PMGI is not a typical EBL resist. Instead, it is commonly used as a lift-off resist in a bilayer stack with PMGI as the bottom layer,⁹ because its chemistry is “orthogonal” to that of the common EBL resist such as PMMA and ZEP-520A. PMGI can be dissolved by basic solutions consisting of KOH or TMAH. As the dissolution rate by a basic solution increases drastically when PMGI is

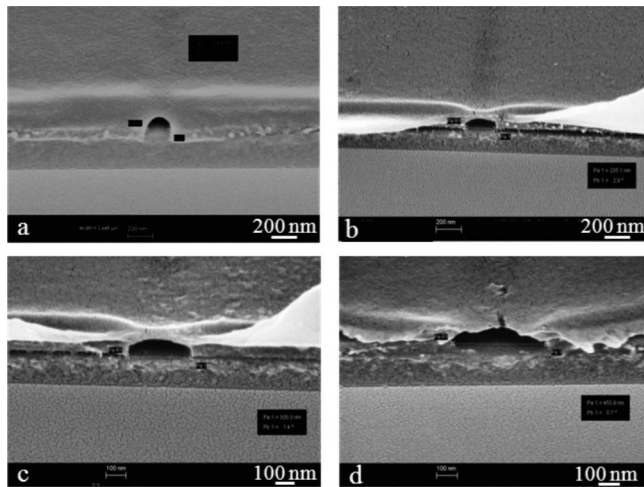


FIG. 3. SEM images showing nanochannels of different widths: (a) 150, (b) 235, (c) 320, and (d) 450 nm.

exposed to e-beam, it is effectively an EBL resist with sensitivity of $50\text{--}100 \mu\text{C}/\text{cm}^2$.^{10,11} However, because it can be dissolved (though very slowly) by its developer even when unexposed, it is not a high resolution resist. Nonetheless, it becomes a high resolution resist with performance comparable to that of PMMA when using solvent developers commonly used for PMMA development such as methyl ethyl ketone and MIBK, though its sensitivity drops considerably to $\sim 1000 \mu\text{C}/\text{cm}^2$ (for 30 keV exposure) when using those developers.^{12,13}

On the other hand, for wider channels, it was found that the process window, noticeably the baking temperature and time, is narrower. Underbaking naturally led to unclosed holes in PMMA, whereas overbaking resulted in the rupture of PMMA membrane, as seen in Fig. 4 for 800-nm-wide channels. We believe that the rupture is mainly caused by the relatively high surface tension of the viscous PMMA, and it would start from a defect or weak point and propagate along the channel. As for the channel depth, here, it is the same as the thickness of the PMGI film (70 nm). Deeper channel would be easier to achieve. For a shallower one, we expect that the chance of the PMMA membrane collapsing onto the ARC surface is still low because the high surface tension of the viscous PMMA would keep the membrane straight above the ARC surface.

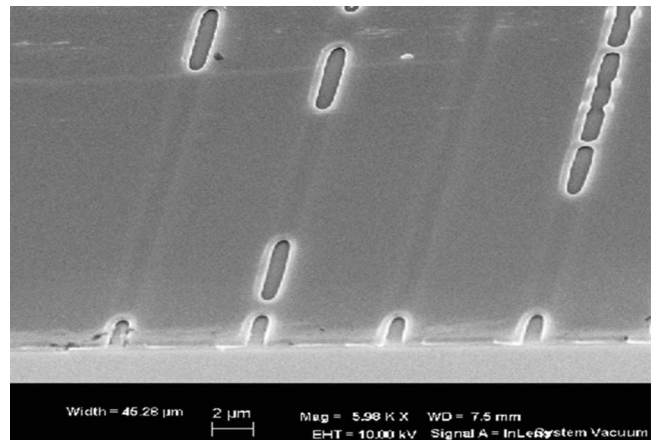


FIG. 4. SEM image showing 800-nm-wide channels with ruptured PMMA membrane.

IV. CONCLUSIONS

Nanofluidic channels were fabricated by electron beam lithography using a bilayer resist of PMMA and PMGI, followed by thermal reflow of PMMA. The current method is simpler than most other approaches for nanochannel fabrication and it does not involve high temperature or high voltage. In addition, it can fabricate channels with various widths and aspect ratios. The current method could find applications in the field of nanofluidics and lab-on-chip devices.

- ¹J. O. Tegenfeldt, C. Prinz, H. Cao, R. L. Huang, R. H. Austin, S. Y. Chou, E. C. Cox, and J. C. Sturm, *Anal. Bioanal. Chem.* **378**, 1678 (2004).
- ²R. B. Schoch, J. Han, and P. Renaud, *Rev. Mod. Phys.* **80**, 839 (2008).
- ³D. Mijatovic, J. C. T. Eijkel, and A. van den Berg, *Lab Chip* **5**, 492 (2005).
- ⁴J. Han and H. G. Craighead, *J. Vac. Sci. Technol. A* **17**, 2142 (1999).
- ⁵H. Cao, Z. Yu, J. Wang, J. O. Tegenfeldt, R. H. Austin, E. Chen, W. Wu, and S. Y. Chou, *Appl. Phys. Lett.* **81**, 174 (2002).
- ⁶X. Chen, R. Ji, M. Steinhart, A. Milenin, K. Nielsch, and U. Gösele, *Chem. Mater.* **19**, 3 (2007).
- ⁷Q. Xia, K. J. Morton, R. H. Austin, and S. Y. Chou, *Nano Lett.* **8**, 3830 (2008).
- ⁸N. R. Devlin, D. K. Brown, and P. A. Kohl, *J. Vac. Sci. Technol. B* **27**, 2508 (2009).
- ⁹Y. Chen, K. Peng, and Z. Cui, *Microelectron. Eng.* **73–74**, 278 (2004).
- ¹⁰H. Takano, H. Nakano, H. Minami, K. Hosogi, N. Yoshida, K. Sato, Y. Hirose, and N. Tsubouchi, *J. Vac. Sci. Technol. B* **14**, 3483 (1996).
- ¹¹B. Cord, C. Dames, K. K. Berggren, and J. Aumentado, *J. Vac. Sci. Technol. B* **24**, 3139 (2006).
- ¹²B. Cui and T. Veres, *Microelectron. Eng.* **85**, 810 (2008).
- ¹³S. M. Saydur Rahman and B. Cui, *Nanoscale Res. Lett.* **5**, 545 (2010).